Adenosine A2A Receptor-Antagonist/Dopamine D2 Receptor-Agonist Bivalent Ligands as Pharmacological Tools to Detect A2A-D2 Receptor Heteromers

Aroa Soriano,[†,▽] Ruben Ventura,[‡,▽] Anabel Molero,[‡] Rob Hoen,[‡] Vicent Casadó,[†] Antoni Cortés,[†] Francesca Fanelli,[§] Fernando Albericio,[‖,⊥,#] Carmen Lluís,[†] Rafael Franco,*,[†] and Miriam Royo*,[‡,#]

[†]*Institut d'Investigacions Biomèdiques August Pi i Sunyer (IDIBAPS), Centro de Investigación Biomédica en Red sobre Enfermedades Neurodegenerativas (CIBERNED), and Department of Biochemistry and Molecular Biology, University of Barcelona, Avenida Diagonal 645, E-08028 Barcelona, Spain,* [‡]*Combinatorial Chemistry Unit, Barcelona Science Park—University of Barcelona, Baldiri Reixac 10, E-08028 Barcelona, Spain,* [§]*Dulbecco Telethon Institute and Department of Chemistry and Advanced Scientific Computing Laboratory, University of Modena and Reggio Emilia, via Campi 183, 41100 Modena, Italy,* [‖]*IRB Barcelona, Barcelona Science Park—University of Barcelona, Baldiri Reixac 10, E-08028 Barcelona, Spain,* [⊥]*Department of Organic Chemistry, University of Barcelona, Martí i Franqués 1-11, E-08028 Barcelona, Spain, and* [#]*CIBER-BBN, Networking Centre on Bioengineering, Biomaterials and Nanomedicine, Barcelona Science Park, Baldiri Reixac 10, E-08028 Barcelona, Spain.* [▽] *These authors have contributed equally to this paper.*

Adenosine A_{2A} ($A_{2A}R$) and dopamine D_2 (D_2R) receptors mediate the antagonism between adenosinergic and dopaminergic transmission in striatopallidal GABAergic neurons and are pharmacological targets for the treatment of Parkinson's disease. Here, a family of heterobivalent ligands containing a D_2R agonist and an $A_{2A}R$ antagonist linked through a spacer of variable size was designed and synthesized to study $A_{2A}R-D_2R$ heteromers. Bivalent ligands with shorter linkers bound to D_2R or $A_{2A}R$ with higher affinity than the corresponding monovalent controls in membranes from brain striatum and from cells coexpressing both receptors. In contrast, no differences in affinity of bivalent versus monovalent ligands were detected in experiments using membranes from cells expressing only one receptor. These findings indicate the existence of $A_{2A}R-D_2R$ heteromers and of a simultaneous interaction of heterobivalent ligands with both receptors. The cooperative effect derived from the simultaneous interaction suggests the occurrence of $A_{2A}R-D_2R$ heteromers in cotransfected cells and in brain striatum. The dopamine/adenosine bivalent action could constitute a novel concept in Parkinson's disease pharmacotherapy.

Introduction

Adenosine A_{2A} and dopamine D_2 receptors belong to the superfamily of G-protein-coupled-receptors (GPCRs[a]). In the

*To whom correspondence should be addressed: Phone: 0034 934021208. Fax: 0034 934021559. E-mail: rfranco@ub.edu. Phone: 0034 934037122. Fax: 0034 934020496. E-mail: mroyo@pcb.ub.cat.

[a] Abbreviations: $A_{2A}R$, adenosine 2A receptor; D_2R, dopamine 2 receptor; $D_{2L}R$, dopamine 2 receptor (long variant); cAMP, cyclic adenosine monophosphate; GPCR, G-protein coupled receptor; GABA, γ-aminobutyric acid L-DOPA, (S)-2-amino-3-(3,4-dihydroxyphenyl) propanoic acid; PEG, polyethylene glycol; XCC, 2-(4-(2,6-dioxo-1,3-dipropyl-2,3,4,5,6,7-hexahydro-1H-purin-8-yl)phenoxy)acetic acid; XAC, 8-(4′-carboxymethoxyphenyl)-1,3-dipropylxanthine-2-aminoethylamide; PPHT-NH2, 6-((4-aminophenethyl)(propyl)amino)-5,6,7,8-tetrahydronaphthalen-1-ol; PPHT, (±)-2-(N-phenethyl-N-propyl)amino-5-hydroxytetralin; AM-MBHA, 2-(4-(amino(2,4-dimethoxyphenyl)methyl)phenoxy)-N-(phenyl(p-tolyl)methyl)acetamide; DIPCDI, N,N′-diisopropylcarbodiimide; PyBOP, benzotriazol-1-yl-oxytripyrrolidinophosphonium hexafluorophosphate; DIEA, diisopropylethylamine; HOBt, hydroxybenzotriazole; HOAt, 1-hydroxy-7-azabenzotriazole; Fmoc, fluorenylmethyloxycarbonyl; TFA, trifluoroacetic acid; Ltk, leukocyte tyrosine kinase; DMSO, dimethyl sulfoxide; RP-HPLC-MS, reversed phase-high performance liquid chromatography—mass spectroscopy; Alloc, allyloxycarbonyl; DMF, dimethylformamide; DBU, diaza(1,3)bicyclo[5.4.0]undecane; DCM, dichloromethane; cDNA, complementary deoxyribonucleic acid; ADA, adenosine deaminase; Tris-HCl, tris(hydroxymethyl)aminomethane hydrochloric acid; Ac2O, acetic anhydride; AcOH, acetic acid; EtOAc, ethyl acetate; DIAD, diisopropyl azadicarboxylate; DCE, 1,2-dichloroethane; THF, tetrahydrofuran; Et3N, triethylamine; PBS, phosphate buffered saline; HEK-293, human embryonic kidney cells; [³H]-YM09151−2, tritium labeled nemonapride (N-(1-benzyl-2-methylpyrrolidin-3-yl)-5-chloro-2-methoxy-4-(methylamino)benzamide); [³H]-ZM241358, tritium labeled 4-(2-[7-amino-2-(2-furyl)-[1,2,4]triazolo[2,3-a][1,3,5]triazin-5-ylamino]ethyl)phenol. Abbreviations used for amino acids follow the IUPAC-IUB Comission of Biochemical Nomenclature in Jones, J. H. *J. Pept. Sci.* **2003**, *9*, 1–8.

last 10 years, several studies have provided solid evidence indicating that GPCRs are expressed on the plasma membrane as homo-, heterodimers, and/or higher-order oligomers.[1−4] These GPCRs heteromers have differential characteristics with respect to the constituting receptors and thus play a significant role in the understanding of receptor function and pharmacology.[5−7] As a result, novel therapies based on GPCR oligomerization have been recently proposed, such as the development of bivalent ligands.[8−10]

$A_{2A}−D_2$ receptor heteromerization has been established in coimmunoprecipitation studies on neuroblastoma cells[11] and by FRET and BRET analysis of living cells.[12,13] $A_{2A}−D_2$ receptor heteromers were found to be constitutive because they were also detected in the absence A_{2A} and D_2 receptor agonist exposure. However, the stoichiometry of $A_{2A}−D_2$ receptor heteromers is unknown and they could represent dimers or high-order oligomers. In addition antagonistic interactions between adenosine $A_{2A}R$ and dopamine D_2R have been determined at the biochemical, functional, and behavioral levels in the striatum, the main input structure of the basal ganglia and a key component of the motor system.[14−16] $A_{2A}R$ and D_2R are colocalized in the dendritic spines of the striatopallidal GABAergic neurons,[17−19] and the activation of $A_{2A}R$ reduces D_2R recognition, G-protein-coupling, and signaling.[20] In the early 1990s, it was proposed that $A_{2A}R$ antagonists should be developed as an anti-Parkinson therapy through their ability to enhance striatal D_2R signaling.[21] In fact, anti-Parkinsonian therapies that combine $A_{2A}R$ selective antagonist and D_2R agonists are currently in clinical trials (phase II).

Adenosine receptor antagonists increase the therapeutic index ratio between the therapeutic and unwanted side effects of L-DOPA and other D_2R agonists.[22,23] In addition, preclinical studies have raised the possibility that these therapies may afford neuroprotective and antidyskinetic benefits.[24]

Despite consistent data providing evidence of heteromerization in heterologous expression systems and indirect evidence of heteromer occurrence in striatal neurons, there is not yet any direct proof of the existence of $A_{2A}-D_2$ receptor heteromers in native tissues. Molecules with the capability to target $A_{2A}-D_2$ receptor heteromers can be functional pharmacological tools to detect heteromers in brain striatum and may also be useful to explore the potential of the $A_{2A}-D_2$ receptor heteromer as a target for Parkinson's disease pharmacotherapy.

Bivalent ligands are defined as molecules that contain two pharmacophores linked through a spacer with the potential to bind simultaneously to the two ligand binding sites present in a GPCR heterodimer. This may result in very high affinity for the receptor and it might allow the targeting of certain heteromeric subtypes, increasing the selectivity of drug action. This approach has been successfully used for some GPCRs leading to interesting results. For instance, Jacobson et al. described heterobivalent ligands composed of an A_1 and A_3 adenosine receptor agonists linked by a spacer that activate both receptors.[25] This coactivation resulted in a cardioprotective effect that is significantly greater than that induced by activation of either receptor individually. Furthermore, opioid-induced tolerance and dependence in mice modulated by the distance between pharmacophores in a bivalent ligand series has been reported by Portoguese et al., a fact that suggests a physical association between μ and δ opioid receptors as heterodimers.[26]

Here we report the design and synthesis of a family of $A_{2A}R$-antagonist/D_2R-agonist heterobivalent ligands as pharmacological tools to study $A_{2A}-D_2$ receptor heteromers. In these compounds, the D_2R agonist and the $A_{2A}R$ antagonist are linked through a spacer of variable length. The spacers were based on trifunctional amino acids in combination with PEG-polyamide unit repeats, and their size was varied (from 26 to 118 atoms) to look for the best interaction with the $A_{2A}-D_2$ receptor heteromer. The binding properties of these compounds were determined by radioligand binding studies in membrane preparations from brain striatum. Furthermore, intracellular cAMP production assays were performed to test the agonistic D_2R and antagonistic $A_{2A}R$ nature of these heterobivalent molecules. Experiments to evaluate the specificity of heterobivalent ligands interaction with $A_{2A}-D_2$ receptor heteromer were performed in cells expressing adenosine and dopamine receptors.

Results

Design of the Libraries. The designed ligands consist of a D_2R agonist and an $A_{2A}R$ antagonist, which are connected by a linker to a variable length spacer. Pharmacophores **1** (XCC), a precursor of xanthine amine congener (XAC),[27] and **2** ((±)-PPHT-NH_2), a derivative of PPHT,[28,29] were chosen as an $A_{2A}R$ antagonist and a D_2R agonist, respectively.

The spacer features a central PEG-polyamide oligomer flanked by adjacent trifunctional amino acid moieties. Trifunctional amino acids were incorporated in the design of the bivalent ligands as linkage moieties to have an easy synthetic connection between the pharmacophore and the

PEG-polyamide oligomer. Spacer length could be varied by changing the number of repetitive PEG-based units ($n = 0-7$) in the central part.

In prior studies, we explored libraries of **1** and **2**, structurally modified with diverse trifunctional amino acids that acted as linkers to optimize the linkage of the pharmacophores to the PEG polyamide based spacer. The most appropriate derivatization for each pharmacophore was chosen on the basis of binding assays and structure−activity relationships.[30] A lysine and a glutamic acid moiety were chosen as linkers for **1** and **2**, respectively.

In addition to the heterobivalent ligand library (compounds **3**−**10**, HXP*n* $n = 0-7$), two libraries of monovalent ligands (compounds **11**−**18**, MX*n* $n = 0-7$) for $A_{2A}R$ and for D_2R (compounds **19**−**26**, MP*n* $n = 0-7$), containing capped linkers, were synthesized as controls in order to factor out possible contributions of the linker to the binding affinity (Figure 1).

Molecular Docking Studies. Docking experiments were performed to confirm that the shortest designed ligand could bind to an $A_{2A}-D_2$ receptor heterodimer. Tridimensional models of the compound and our previously reported $A_{2A}-D_2$ receptor heterodimer model[12] were used in these experiments. In this model, the heterodimer interface is mainly formed by the second intracellular loop (I2), helices 4, 3, and 5 from D_2R, and I2, helices 5, 3, and 4 from $A_{2A}R$. The estimated maximum inter-Cα distance between the two binding pockets of the receptors that participate in the dimer is in the range of 40−45 Å. These distances did not account for the presence of additional lipids or domain swapping. The linkers synthesized varied from 26 atoms (**3**) to 118 atoms (**10**) and were characterized for being hydrophilic and highly flexible (Figure 1). Compound **3** with the linker (Lys-Lys-[PEG/polyamide]$_0$-Lys-Glu) was manually docked into the putative binding sites of the two receptors by probing slightly different conformations of the ligand and the receptor side chains. The complex in Figure 1 in the Supporting Information (SI) shows tight binding for compound **3** with all three positively charged groups of the ligand interacting with anionic amino acids and with most of the heteroatoms of the ligand involved in H-bonds with the receptor. In this complex, different from the XCC adenosinic pharmacophore, the PPHT head performs specific interactions with D_2R. Such interactions, which consist of the H-bonds between the protonated nitrogen atom and the hydroxy group of the ligand and, respectively, D114 and S197 of the receptor, are consistent with the agonistic nature of PPHT. The docking study predicts that even when the shortest bivalent ligand adopts a partially extended conformation, it can be enough to allow the two pharmacophoric parts to bind to an $A_{2A}-D_2$ receptor heterodimer. However, due to the flexibility of the linker part, we decided to explore other ligand lengths.

Synthesis of the Different Building Blocks of the Library. The synthesis of the pharmacophores **1** and **2** is described in Schemes 1 and 2, respectively. Compound **1** could be obtained over five steps starting from the commercially available 1,3-dipropyl-urea (**27**) and cyano acetic acid (**28**). Condensation of urea **27** with cyano acetic acid followed by ring closure under basic conditions gave 1,3-dipropylpyrimidine-2,4(1*H*,3*H*)-dione (**29**) in 60% yield over two steps. Uracil **31** was obtained in 38% yield over two steps by nitrite addition to **29** and subsequently reduction of the nitrite functionality to an amine. Finally, the two-step
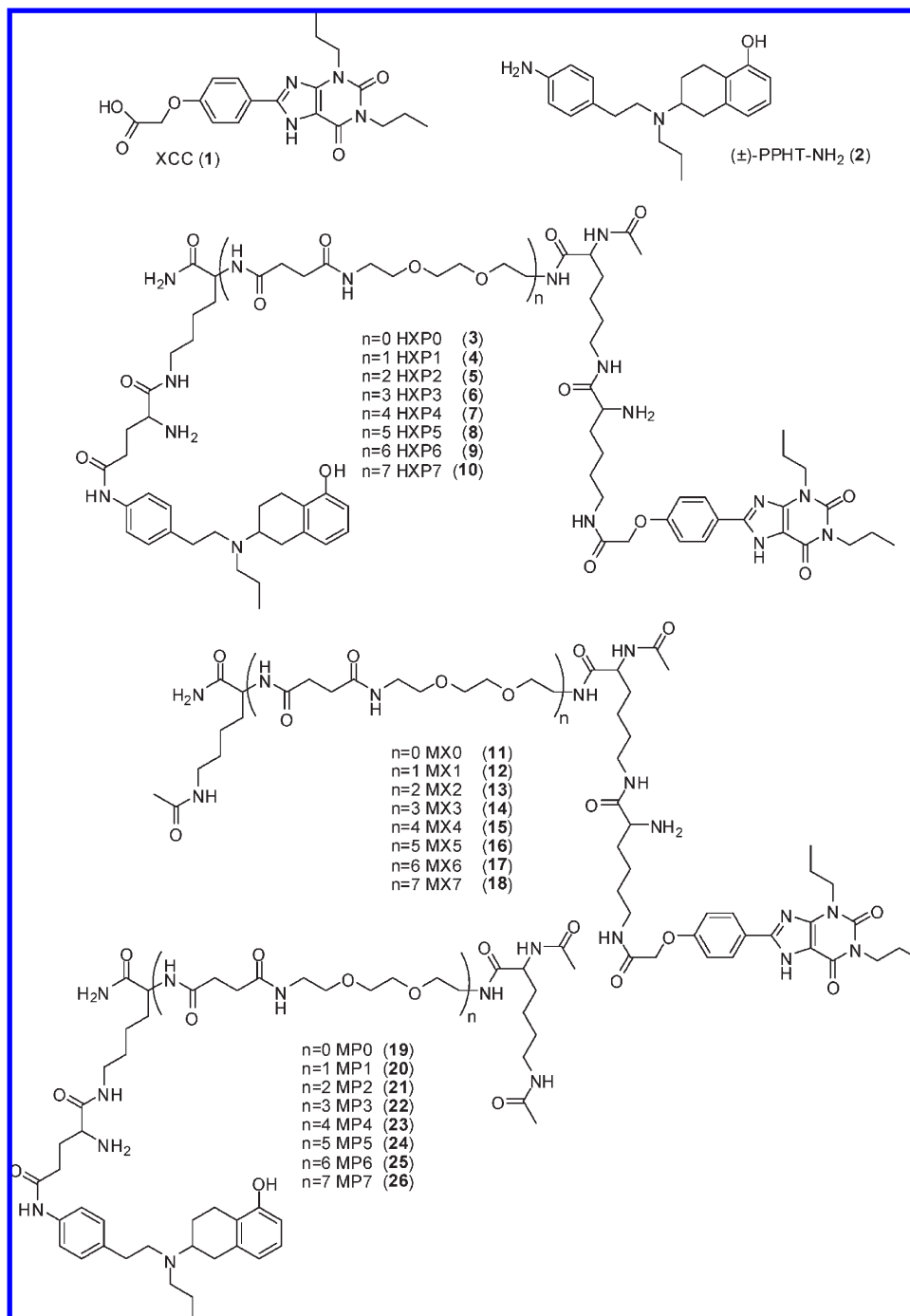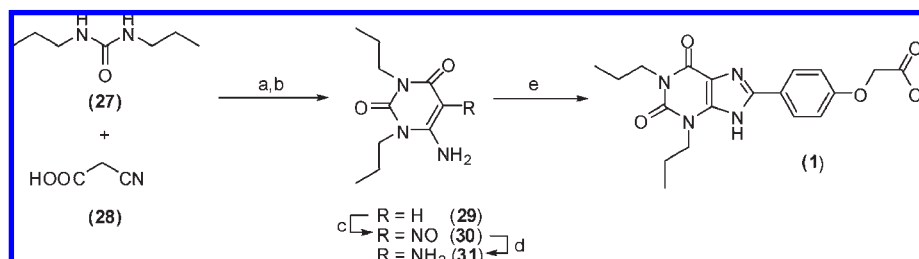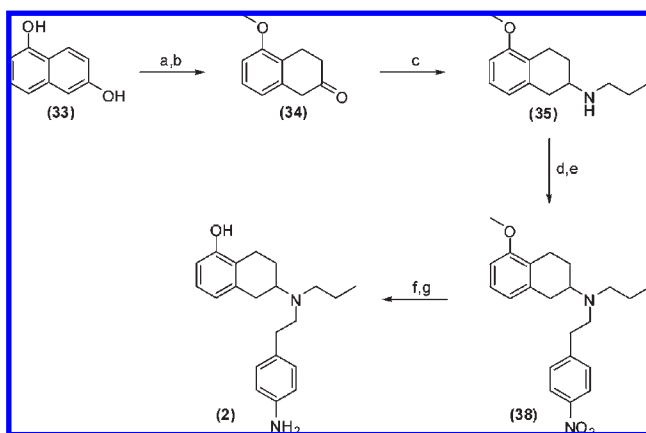
Figure 1. Designed mono- and heterobivalent ligands.

Scheme 1. Synthesis of **1**[a]

[a] (a) Ac₂O, 80 °C, 90%; (b) 70% NaOH$_{(aq)}$, pH 10−11, 67%; (c) NaNO₂, 42% AcOH$_{(aq)}$, 52%; (d) Na₂S₂O₄, EtOAc/H₂O, 74%; (e) 2-(4-formylphenoxy)acetic acid (**32**), EtOH, AcOH, Δ, then DIAD, toluene, Δ, 54%.

Scheme 2. Synthesis of **2**[a]

[a] (a) Me$_2$SO$_4$, K$_2$CO$_3$, acetone, Δ, 94% (b) EtOH, Na, 50 °C to Δ, then conc. HCl$_{(aq)}$, Δ 88% (c) DCE, NaBH(OAc)$_3$, 67% (d) 2-(4-nitrophenyl)acetyl chloride (**36**), Et$_3$N, DCM, RT, 87% (e) 1M BH$_3$·THF in THF, 0 °C to Δ, 67% (f) H$_2$NNH$_2$, Raney-Ni, EtOH, Δ, 74% (g) 1M BBr$_3$ in DCM, −78 °C to RT, 85%.

condensation of uracil **31** with 2-(4-formylphenoxy)acetic acid (**32**) was performed to give the final product **1** in 54% yield. Most of the products were easy to purify because they were insoluble in the reaction solvents. Simple filtration and subsequent drying of the solid gave the desired products in good to excellent yields with high purities.

Compound **2** was synthesized in a slightly different route compared to an earlier published synthesis.[28] Etherification of the commercially available 1,6-dihydroxynaphthalene (**33**) followed by a Birch reduction gave 5-methoxy-2-tetralone (**34**) in an 83% yield over two steps. Reductive amination of **34** with propyl amine and NaBH(OAc)$_3$ as reductive agent yielded the secondary amine **35** in a good yield. Reaction of **35** with acid chloride **36** gave amide **37** as a 1:1 mixture of two rotamers as could be observed by ^{1}H and ^{13}C NMR. Subsequent reduction of the amide functionality with a 1 M solution of BH$_3$·THF complex in THF yielded **38** in 58% over two steps. Reduction of the NO$_2$ group with hydrazine and Raney-Ni followed by deprotection of the methyl ether by a BBr$_3$ solution in DCM gave the desired PPHT-NH$_2$ (**2**) in a 63% yield. All products were characterized by standard techniques such as ^{1}H and ^{13}C NMR and HPLC-MS.

The monomeric PEG-based unit (**39**) was synthesized according to a previously described procedure.[31]

Synthesis of the Libraries. The synthesis of the libraries of heterobivalent and monovalent ligands was carried out by an Fmoc-based solid-phase strategy using the AM-MBHA resin as a polymeric support (Scheme 3). The amino acids were coupled under standard peptide coupling conditions using DIPCDI or PyBOP/DIEA as coupling reagents and HOBt or HOAt as additives. Initial coupling of a Fmoc-Lys(Alloc)-OH to the resin and subsequent selective removal of the Fmoc-protecting group was followed by coupling of a monomeric Fmoc-PEG-based unit (**39**). The process of Fmoc elimination and coupling of a new monomeric Fmoc-PEG-polyamide unit was repeated to construct diverse length spacers ($n = 0$–7). Further construction of the ligands is depicted in Scheme 3. Whereas the **1** and its corresponding lysine linker were introduced separately into the ligands, **2** and its glutamic acid linker were introduced as one building block, previously synthesized by coupling of **2** to Fmoc-Glu(*t*-Bu)-OH with a subsequent *t*-Bu ester

hydrolysis. After the synthesis was completed, the ligands were cleaved from the solid support with TFA/H$_2$O (95:5). Purification of the ligands was done by preparative HPLC, yielding high purity ligands (≥95%).

**Binding Properties of Bivalent and Monovalent Ligands.** The binding properties of heterobivalent ligands **3**−**10** and monovalent ligands **11**−**26** were assayed via competitive radioligand experiments using brain striatal membranes given the fact that D$_2$R and A$_{2A}$R are naturally coexpressed in striatal neurons.[32] The A$_{2A}$R selective antagonist [3H]-ZM241385 was used to evaluate the binding properties of heterobivalent ligands **3**−**10** and monovalent ligands **11**−**18** to this receptor (Figure 2a). XAC was tested as a reference compound showing that the introduction of linkers to the pharmacophore leads to a reduction in the displacement of the radioligand binding to A$_{2A}$R. As predicted, the binding of monovalent ligands decreased when the ligand spacer length increased. To illustrate this, the shortest ligand **11** exhibited a radioligand binding decrease of 58%, compared to the longest ligand **18** that showed a radioligand binding decrease of 17%. All heterobivalent ligands showed greater capacity to displace specific [3H]-ZM241385 binding than the corresponding monovalent ligands. Heterobivalent ligands **3**−**6**, with linkers from 26 to 66 atoms, competed with the [3H]-ZM241385) with similar results, showing approximately a radioligand binding decrease of 70% and higher radioligand binding displacement than longer bivalent compounds.

A similar competition experiment was performed using the D$_2$R antagonist [3H]-YM09151-2 (Figure 2b) as radioligand to evaluate the binding properties of these ligands for D$_2$R. In these assays, heterobivalent ligands **3**−**10** exhibited higher displacement of specific [3H]-YM09151-2 binding than the corresponding monovalent compounds **19**−**26** without any clear influence of the spacer length. A reduction in the binding of these ligands for D$_2$R was detected when compared with the reference control (±)PPHT binding, however no significant differences in the binding properties were found between members of the same library (monovalent or heterobivalent ligands).

Binding Affinities of the Selected Ligands. After screening, shorter heterobivalent ligands **3**−**6**, that exhibited higher displacement of specific A$_{2A}$R radioligand binding and the corresponding monovalent compounds **11**−**14** and **19**−**22** were selected to determine their pharmacological profiles.

Competition experiments in brain striatal membranes were performed using 2.1 nM [3H]-ZM241385 for the A$_{2A}$R binding or 0.9 nM [3H]-YM09151-2 for the D$_2$R binding and increasing concentrations of heterobivalent and monovalent compounds and for the control competition experiments increasing concentrations of ZM-241385 for A$_{2A}$R or YM-09151-2 for D$_2$R. Representative competition curves for compounds **6**, **14**, and **22** are shown in Figure 3a. Considering the existence of homodimers of A$_{2A}$R[33] and homodimers of D$_2$R,[34] binding data were fitted to the two-state dimer receptor model[35−37] to calculate macroscopic equilibrium dissociation constants (K_{DB1} and K_{DB2}) and the binding cooperativity evaluated as the cooperative index D_C (Table 1). Competition curves were biphasic for the D$_2$R binding showing negative cooperativity (negative D_C values) arising from molecular communication between the two subunits of the receptor homodimer (Figure 3b). Monophasic competition curves were obtained for A$_{2A}$R binding, indicating cooperativity 0; that means compounds bind with the same affinity to the two subunits in the A$_{2A}$R homodimer and therefore K_{DB1} is enough to characterize the binding (Figure 3a).[38]

Scheme 3. Synthetic Procedure for Heterobivalent Ligands (**3**−**10**) and Their Corresponding Monovalent Ligands (**11**−**18**, **19**−**26**)[a]
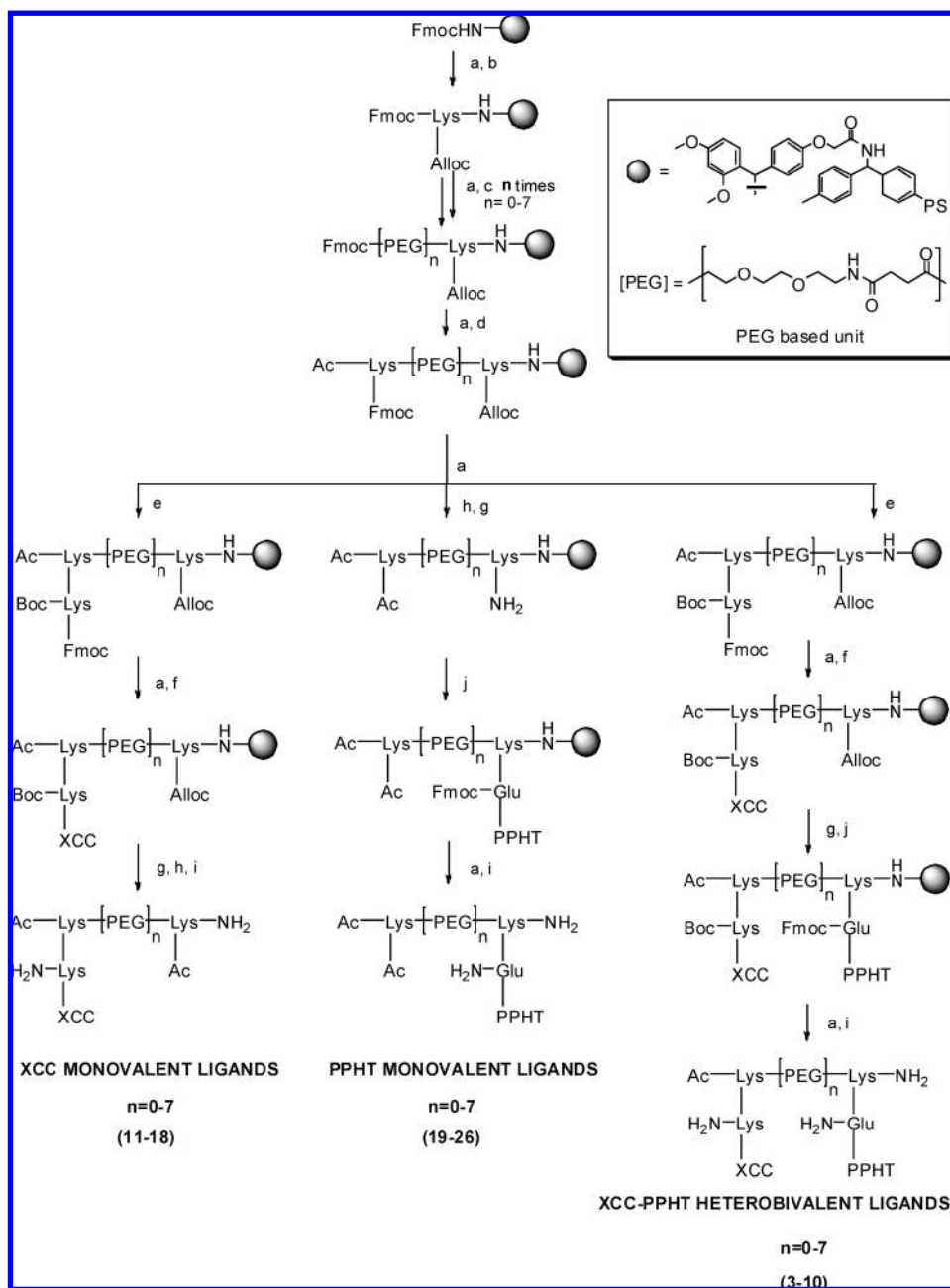

[a] Conditions: (a) 1:4 or 1:1 piperidine in DMF; (b) Fmoc-Lys(Alloc)-OH, DIPCDI/HOBt; (c) Fmoc-HN(PEG)-OH, PyBOP, HOAt, DIEA; (d) Ac-Lys(Fmoc)-OH, PyBOP, HOAt, DIEA; (e) Boc-Lys(Fmoc)-OH, PyBOP, HOAt, DIEA; (f) **1**, PyBOP, HOAt, DIEA; (g) Pd(PPh$_3$)$_4$-PhSiH$_3$ in DCM$_{anh}$; (h)Ac$_2$O, DIEA; (i) TFA-H$_2$O (95:5); (j) Fmoc-Glu(PPHT)-OH, PyBOP, HOAt, DIEA.

In agreement with the results obtained in the screening, the A$_{2A}$R binding affinity of xanthine-derived monovalent ligands decreased with increasing ligand length (from 160 to 364 nM). In contrast, irrespective of linker length, heterobivalent ligands displayed similar affinities for A$_{2A}$R (50 to 80 nM). The affinity was 3−7 times higher for heterobivalent compounds compared to their monovalent counterparts (Table 1, column 3). Taking into account the values of K_{DB1} and K_{DB2} for D$_2$R, compounds **5** and **6** showed the highest binding enhancement (7−18 fold increase). For D$_2$R binding, no correlation was observed between linker length and binding affinity of the compounds.

Heterobivalent Ligand Capacity to Detect A$_{2A}$−D$_2$ Receptor Heteromers. To confirm the specific interaction of

heterobivalent ligands with A$_{2A}$−D$_2$ receptor heteromers and consequently validate their capacity to detect these heteromers in native tissue, competition experiments were performed using membrane preparations from Ltk cells expressing human A$_{2A}$R, human D$_2$R, or both receptors. Representative screening of heterobivalent compounds **4** and **6** and their corresponding monovalent ligands **12**, **14**, **20**, and **22** are shown in Figure 4.

In membranes from cells that coexpressed D$_2$R and A$_{2A}$R, heterobivalent ligands displayed higher displacement of the radioligand [^{3}H]ZM-241385 binding than that of the monovalent counterparts (MX$_n$). Nevertheless, when only A$_{2A}$R was expressed the same radioligand displacement was observed for heterobivalent and monovalent ligands alike (Figure 4a,b). In the case of D$_2$R,
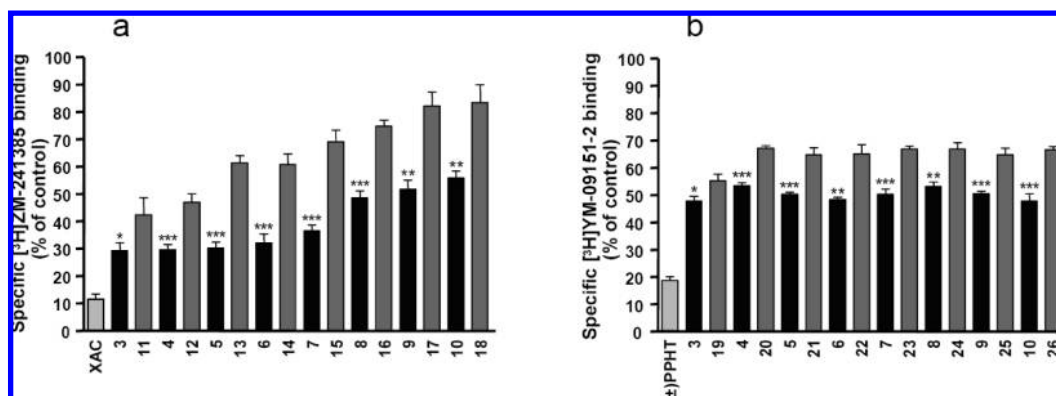
Figure 2. Screening of heterobivalent (black bars) and monovalent (gray bars) compounds using striatal membranes. (a) Displacement of $A_{2A}R$ selective antagonist [^{3}H]ZM-241385 (2.3 nM) binding by XAC and by heterobivalent **3−10** and monovalent **11−18** compounds. (b) Displacement of D_2R antagonist [^{3}H]YM09151-2 (1.2 nM) binding by (±)PPHT and by heterobivalent **3−10** and monovalent **19−26** compounds. The concentration of the different molecules was 1 μM. Values are given as % of control (specific radioligand binding determined in the absence of displacer). Data are mean ± SD of three independent experiments. Heterobivalent ligand significantly different (*$p < 0.05$, **$p < 0.005$, ***$p < 0.0005$) vs the corresponding monovalent ligand by Student's t test for unpaired samples.
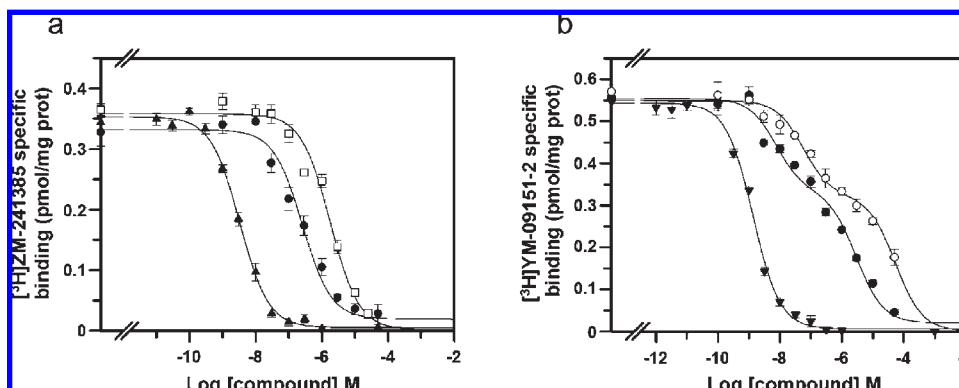
Figure 3. Representative competition curves for compounds **6** (●), **14** (□), and **22** (○) in striatum membranes. (a) Compounds **6** (●) and **14** (□) or ZM 241358 (▲) competed with 2.1 nM [^{3}H] ZM241358. (b) Compounds **6** (●) and **22** (○) or YM09151−2 (▼) competed with 0.9 nM [^{3}H]-YM09151-2. Data are means ± SD from representative experiments performed in triplicate.

Table 1. Binding Affinity of Heterobivalent and Monovalent Ligands to $A_{2A}R$ and D_2R in Brain Striatum Membranes[a]

linker and length	ligand	K_{DB1} (nM)	D_C	ligand	K_{DB1} (nM)	K_{DB2} (μM)	D_C
		$A_{2A}R$			D_2R		
(Lys-Lys-[PEG/polyamide]$_0$-Lys-Glu)	**3**	55 ± 9	0	**3**	1.0 ± 0.2	9 ± 2	−3.3
26 atoms	**11**	160 ± 17	0	**19**	4 ± 1	9 ± 2	−2.8
(Lys-Lys-[PEG/polyamide]$_1$-Lys-Glu)	**4**	59 ± 11	0	**4**	1.1 ± 0.3	7 ± 3	−3.2
40 atoms	**12**	246 ± 37	0	**20**	11 ± 2	15 ± 5	−2.5
(Lys-Lys-[PEG/polyamide]$_2$-Lys-Glu)	**5**	80 ± 10	0	**5**	1.1 ± 0.3	1.4 ± 0.5	−2.5
53 atoms	**13**	268 ± 40	0	**21**	11 ± 2	12 ± 3	−2.5
(Lys-Lys-[PEG/polyamide]$_3$-Lys-Glu)	**6**	50 ± 8	0	**6**	1.8 ± 0.4	0.5 ± 0.1	−1.8
66 atoms	**14**	364 ± 45	0	**22**	13 ± 3	9 ± 2	−2.2

[a] Results are given as parameter values ± SEM of three independent experiments. K_{DB1} and K_{DB2} are, respectively, the equilibrium dissociation constants of the first (high affinity) and second (low affinity) binding of ligand to the dimeric $A_{2A}R$ or D_2R. Because $A_{2A}R$ is non-cooperative, in this case, K_{DB2} is $4K_{DB1}$. D_C is the dimer cooperativity index for the binding of ligand.[37]

similar results were observed; heterobivalent ligands showed higher displacement of the radioligand binding than that of the corresponding monovalent compounds when D_2R and $A_{2A}R$ are coexpressed, but when only D_2R was expressed were no differences found in the displacement of radioligand [^{3}H]-YM09151-2 binding (Figure 4c,d). The binding of [^{3}H]-YM09151-2 or [^{3}H]ZM-241385 was not affected by MX$_n$

or MP$_n$ monovalent ligands, respectively, in cells expressing D_2R or $A_{2A}R$, respectively (data not shown).

In conclusion, heterobivalent ligands (**4** and **6**) showed a different behavior in both receptors when $A_{2A}-D_2$ receptor heteromers are present increasing their capacity to displace the radioligands compared to their corresponding monovalent ligands (**12**, **14**, **20**, and **22**). As we explained before, this
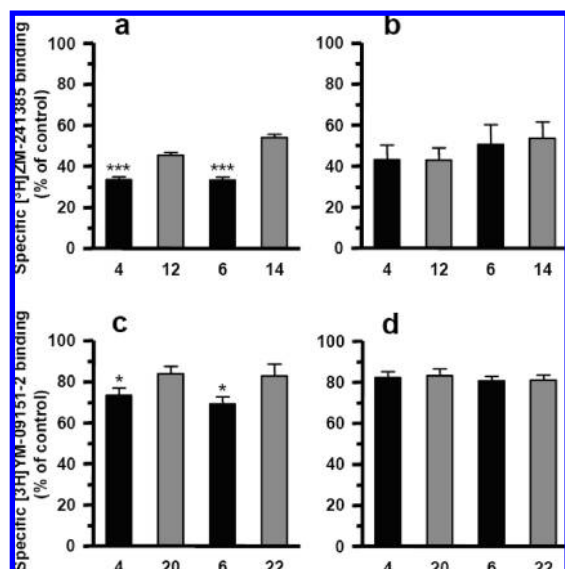
Figure 4. Interaction of heterobivalent ligands with $A_{2A}-D_2$ receptor heteromers. Competition experiments of $A_{2A}R$ selective antagonist [^{3}H]ZM-241385 (2.1 nM) vs heterobivalent **4** and **6** and monovalent **12** and **14** compounds using membrane preparations from mouse fibroblast Ltk cells coexpressing $A_{2A}R$ and D_2R (a) or expressing $A_{2A}R$ (b). Competition experiments of D_2R antagonist [^{3}H]YM09151-2 (1.9 nM) vs heterobivalent **4** and **6** and monovalent **20** and **22** compounds using membrane preparations from mouse fibroblast Ltk cells coexpressing $A_{2A}R$ and D_2R (c) or expressing D_2R (d). The concentration of the different molecules was 1 μM. Values are given as % of control (specific radioligand binding determined in the absence of displacer). Data are mean $\pm$ SD of three independent experiments. Heterobivalent ligand was significantly different (*$p < 0.05$, **$p < 0.005$, ***$p < 0.0005$) compared to the corresponding monovalent ligand by Student's t test for unpaired samples.

effect was also detected in native tissue that coexpressed both receptors as brain striatal membranes. However, in the absence of $A_{2A}-D_2$ receptor heteromers and when both receptors were in their monomeric or homodimeric form, no differences were detected between heterobivalent and monovalent ligands. This fact demonstrates the specific interaction of these heterobivalent ligands with $A_{2A}-D_2$ receptor heteromers and makes these ligands useful as pharmacological tools to detect receptor heteromers in native tissue.

$A_{2A}R$ Antagonist and D_2R Agonist Heterobivalent Ligand Behavior. Bivalent drugs useful for Parkinson's disease would act as agonists for D_2R and as antagonists for $A_{2A}R$. Activated $A_{2A}R$ couples to Gs protein, which leads to the activation of adenylate cyclase and therefore to an increase in cAMP levels. On the contrary, D_2R activation results in coupling to Gi proteins, which leads to the inhibition of adenylate cyclase and as a result to a decrease in cAMP levels. To find out the functional properties of heterobivalent ligands, cAMP determination assays were performed. In these assays, it was not possible to evaluate whether the designed bivalent ligands behaved as $A_{2A}R$ antagonists and D_2R agonists at the same time. For this reason, human D_2R and human $A_{2A}R$ were expressed separately in HEK cells. Because receptors were singly expressed, heterobivalent ligands bound to $A_{2A}R$ or to D_2R in a monovalent mode. These ligands did not act as $A_{2A}R$ agonists because they did not increase basal cAMP levels (Figure 5a). In these experiments, bivalent ligands **4**
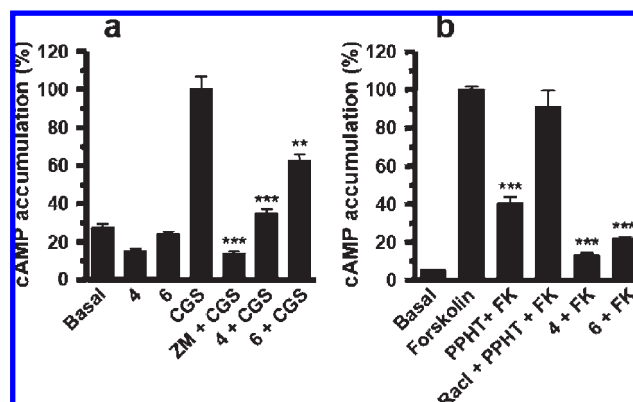
Figure 5. cAMP assays. (a) HEK-293 cells expressing the human $A_{2A}R$ were treated with 200 nM of the $A_{2A}R$ specific agonist CGS 21680 (CGS) and/or 10 μM of the $A_{2A}R$ antagonist ZM 241385 (ZM), 10 μM **4**, or 10 μM **6**. Results are presented as % of cAMP accumulation achieved after treatment with the agonist, CGS 21680. (b) HEK-293 cells expressing the human D_2R were treated with 10 μM forskolin in the presence of: 1 μM of the D_2R agonist ($\pm$)PPHT, 30 μM of the D_2R antagonist raclopride (Racl) plus 1 μM ($\pm$)PPHT, 10 μM **4**, or 10 μM **6**. Results are presented as % of cAMP accumulation achieved after treatment with forskolin. "Basal" represents cAMP levels in nonstimulated cells. Results are mean $\pm$ SD of three independent experiments. (Student's t-test showed significant cAMP decreases in relation to treatment with CGS 21680 in (a) or in relation to forskolin treatment in (b): **$p < 0.001$ and ***$p < 0.0001$).

and **6** antagonized CGS21680-induced cAMP production and therefore they behaved as $A_{2A}R$ antagonists. As anticipated, given that the selective antagonist ZM241385 used as a control had a higher affinity than xanthine congeners and that the introduction of the linker to the pharmacophore most likely decreased the affinity, heterobivalent ligands were less potent than ZM241385. Because D_2R couple to Gi proteins, the efficacy of 10 μM of heterobivalent ligands to decrease cAMP levels was tested in forskolin-treated cells (Figure 5b). Compounds **4** and **6** conserved the ($\pm$)PPHT agonistic character, causing, respectively, an 87% and a 78%, decrease in the forskolin-induced cAMP levels .

Discussion

GPCRs dimer/oligomer formation influences receptor function and pharmacology and has an important impact on GPCR drug design.[8,10,39] The development of bivalent ligands that target GPCR dimers is an approach for the study of GPCR oligomerization and for the design of novel therapies. Several reports have described the application of the "bivalent ligand" approach for the oligomerization study of a variety of GPCRs including δ/κ opioid,[40,41] 5-HT(1B/1D), and 5-HT(4) homodimers serotonin,[42,43] as well as muscarinic-acetylcholine[44] and melanocortin-4/δ-opioid[45] receptors.

In the present study, we synthesized a library of heterobivalent ligands constituted by two pharmacophoric moieties, XCC (**1**) as $A_{2A}R$ antagonist and ($\pm$)-PPHT-NH$_2$ (**2**) as D_2R agonist, that are connected via Lys-Lys-[PEG/polyamide]$_n$-Lys-Glu ($n = 0-7$) linkers. These compounds showed a greater capacity to displace specific $A_{2A}R$ and D_2R radioligand binding than their corresponding monovalent controls when both receptors were present in brain striatum membranes.

Monovalent ligands, containing one pharmacophore with matched spacers, were tested in brain striatum tissue to determine whether a change in spacer length influenced ligand

binding. In this regard, the incorporation of the linker to the pharmacophore led to a decrease in the displacement of the radioligand binding. The capacity of xanthine-derived monovalent ligands to displace [^{3}H]-ZM241385 in A$_{2A}$R decreased with increasing ligand molecular weight. In contrast, no correlation was observed between linker length and binding to D$_2$R of (±)PPHT-derived monovalent compounds.

Shorter heterobivalent ligands with linkers Lys-Lys-[PEG/polyamide]$_n$-Lys-Glu $n = 0–3$ exhibited higher displacement of specific A$_{2A}$R radioligand binding. As predicted by preliminary docking experiments (see SI Figure 1), the shortest linker (26 atoms) is long enough to allow the two pharmacophoric moieties to bind to an A$_{2A}$–D$_2$ receptor heterodimer. The estimated maximum inter-Cα distance between the two binding pockets of the receptors that participate in the dimer is in the range of 40–45 Å. This range is similar to the one proposed in recent studies for other receptor dimers, including opioid receptors,[40] serotonin 5-HT$_4$ receptor,[43] and human melanocortin receptor 4.[46] Our estimations, which had been based on the complex between compound **3** and a D$_2$R–A$_{2A}$R heteromer model previously built,[12] found support in a couple of alternative complexes involving two alternative heterodimer models (see SI Figures 1–3). The latter are made by two variances of a novel D$_2$R model based upon the crystal structure of the β_2-adrenergic receptor[47] (β_2-AR) (PDB code: 2RH1), on one hand, and the very recently released crystal structure of A$_{2A}$R[48] (PDB code: 3EML), on the other one. Although the intermonomer interfaces vary in the three different heterodimers, the two pharmacophoric moieties of **3** dock into the same receptor sites. This is particularly true for the D$_2$R moiety that experiences the H-bonds with D114 in helix 3 and with either S193 or S197 in helix 5 (see SI Figures 1–3).

The pharmacological characterization of heterobivalent ligands with Lys-Lys-[PEG/polyamide]$_n$-Lys-Glu ($n = 0–3$) linkers was performed in brain striatum tissue by means of competition experiments using radiolabeled A$_{2A}$R or D$_2$R antagonists and increasing concentrations of heterobivalent ligands. To calculate receptor affinity for heterobivalent ligands, the previously described two-state dimer receptor model was used to fit binding data.[37] The K_{DB1} and K_{DB2} values reported here are the macroscopic dissociation constants describing the binding of the first and the second ligand molecule to the homodimeric receptor. While competition curves of [^{3}H]-YM09151-2 vs heterobivalent ligands **3–6** or monovalent ligands **19–22** were biphasic, those corresponding to [^{3}H]-ZM241385 vs heterobivalent ligands **3–6** or monovalent ligands **11–14** were monophasic. The cooperativity index values obtained indicated negative cooperativity in ligand binding for D$_2$R but not for A$_{2A}$R.

Heterobivalent ligands **3–6** with linker lengths ranging from 26 to 66 atoms displayed similar binding affinities for A$_{2A}$R (between 50 ± 8 and 80 ± 10 nM), which were 3–7 times higher compared to those of their monovalent counterparts **11–14**. Recent computational modeling has revealed that similar PEG/polyamide based linkers could assume multiple conformations, from linear to curved, with a wide range of distances.[46] The high flexibility of the Lys-Lys-[PEG/polyamide]$_n$-Lys-Glu linker likely explains the lack of correlation between linker length and binding affinity. For D$_2$R, heterobivalent ligands **3–6** exhibited higher binding affinities (1.0 ± 0.2 to 1.8 ± 0.4 nM for K_{DB1}) compared to that of their corresponding monovalent ligands **19–22** but again showing no correlation with linker length. Taking into account dissociation constant values (K_{DB1} and K_{DB2}), compounds **5** and **6** showed the highest binding affinity enhancement (7–18 fold increase) for D$_2$R.

To bear out the specific interaction of the two pharmacophoric parts of the bivalent ligand with the A$_{2A}$–D$_2$ receptor heteromer, competition binding assays were performed using membrane preparation from Ltk cells expressing human A$_{2A}$R or human D$_2$R or both receptors at the same time. The results revealed that it was only when both receptors were coexpressed that bivalent ligands showed higher displacement of specific radioligand binding than monovalent ligands. Thus the high affinity of heterobivalent ligand versus monovalent ligands is only observed in cells coexpressing both receptors, indicating a simultaneous interaction of heterobivalent ligands with D$_2$R and A$_{2A}$R. This high affinity is difficult to be explained without considering a significant concentration factor exerted by heterobivalent ligands that can be considered an indicator of A$_{2A}$–D$_2$ receptor heteromers existence. This effect was also observed when the binding experiments were carried out with brain striatum tissue as described above and could be indicative of the existence of A$_{2A}$–D$_2$ receptor heteromers in native brain membranes.

Taken all together, these results indicate that a heterobivalent ligand bound to D$_2$R may subsequently bind to A$_{2A}$R located in the vicinity with a higher affinity than the corresponding A$_{2A}$R monovalent ligand. Similarly, a heterobivalent compound bound to A$_{2A}$R subsequently binds to D$_2$R located in closer proximity with a higher affinity than its D$_2$R monovalent counterpart. This in turn indicates a significant concentration factor exerted by heterobivalent ligands that can be considered only if both receptors are in a very close proximity. Thus, dopamine–adenosine heterobivalent ligands are useful tools to show the occurrence of these heteromers in brain striatum and the increased affinity of these ligands detected when both receptors are present is a strong indication of binding to A$_{2A}$–D$_2$ receptor heteromers.

Although powerful biophysical techniques such as fluorescence resonance energy transfer (FRET) and bioluminescence resonance energy transfer (BRET) have been decisive in demonstrating heteromer formation in heterologous expression systems, the demonstration of occurrence of dimers in natural tissues is still a matter of controversy. Coimmunoprecipitation of two receptors is not considered proof of heteromerization due to the fact that the result may be a detergent-induced membrane protein aggregation process.[49] Heterobivalent ligands are valuable pharmacological tools that allow demonstration of the existence of A$_{2A}$–D$_2$ receptor heteromers even in native tissue and can be used to study a specific GPCR dimer behavior without any receptor modification. Furthermore, heterobivalent ligands strategies can be developed to identify heteromers that involve other neurotransmitter and/or neuromodulator receptors, which may lead to novel therapeutic approaches to combat a variety of neurological and neuropsychiatric diseases.

In summary, in the present work, we designed and synthesized heterobivalent ligands that serve as a probe for A$_{2A}$D$_2$ receptor heteromers in native tissues and could open new avenues for the design of heteromer-selective drugs for treatment of Parkinson's disease.

Experimental Section

Materials and Equipment. All chemical reagents were obtained from commercial suppliers and used without further

purification. Melting points were determined on a Buchi melting point B-549 apparatus. ^{1}H and ^{13}C NMR spectra were recorded at 298 K on a Varian Mercury-400 Fourier transform spectrometer. Chemical shifts are reported in δ units (ppm) relative to the residual deuterated solvent signals of CHCl$_3$ (^{1}H NMR: δ 7.26; ^{13}C NMR: δ 77.0), DMSO (^{1}H NMR: δ 2.49; ^{13}C NMR: δ 39.5). The splitting patterns are designated as follows: s (singlet), d (doublet), t (triplet), q (quartet), b (broad). The RP-HPLC analyses were performed on a Waters Alliance instrument and RP-HPLC-MS on a Waters Alliance instrument coupled to a Micromass ZQ spectrometer with an electrospray (ES) probe. The purifications by preparative RP-HPLC were performed on a Waters HPLC autopurification FractionLynx UV/MS system with an electrospray (ES) probe. Analytical thin-layer chromatography (TLC) was performed on precoated plates (Merck silica gel 60ACC, F254). Visualization of the developed chromatogram was achieved with UV light. Manual flash column chromatography was performed using silica (Merck, 70–230 mesh). Automated flash chromatography was performed on a Teledyne Isco module companion with photodiode array detector using Silica-RediSep columns.

Dulbecco's modified Eagle's medium (DMEM), sodium pyruvate, L-glutamine, penicillin/streptomycin, FBS, and Lipofectamine 2000 were purchased from Invitrogen (Grand Island, NY). Adenosine deaminase (ADA) EC 3.5.4.4 was supplied by Roche (Basel, Switzerland), and bicinchoninic acid method was supplied by Pierce Chemical Co (Rockford, IL). Protease inhibitor cocktail, raclopride, (±)-PPHT, and forskolin were purchased from Sigma (St. Louis, MO). [^{3}H]- ZM 241385 was purchased from American Radiolabeled Chemicals (St. Louis, MO). ZM241385, CGS 21680, and zardaverine were supplied by Tocris Biosciences (Avonmouth, UK). [^{3}H]-YM 09151-2 was supplied by PerkinElmer (Boston, MA). Ecoscint H scintillation cocktail was purchased from National Diagnostics (Atlanta, GA) and Cyclic AMP (3H) Assay system from Amersham Biosciences (Uppsala, Sweden). Membranes were homogenized with Polytron homogenizer (PTA 20 TS rotor, setting 3; Kinematica, Basel, Switzerland). Radioligand binding experiments were performed using a Brandel cell harvester (Gaithersburg, MD) and a Packard 1600 Tri-Carb scintillation counter. GRA-FIT was supplied by Erithacus Software (Surrey, UK).

Solid-Phase Synthesis. All solid-phase syntheses were carried out manually in a polypropylene syringe fitted with a polyethylene porous disk. Solvents and soluble reagents were removed by suction. Peptide synthesis for this work employed a combined Fmoc/Alloc/tBu solid phase strategy on a Fmoc-AM-MBHA resin. Washings between deprotection, coupling, and subsequent deprotection steps were carried out with DMF (5 × 1 min) and DCM (5 × 1 min) using 10 mL of solvent/g of resin each time. All the couplings and Fmoc removal were monitored using the Kaiser test.

Fmoc Group Removal. Fmoc group removal involved the following sequence: (i) DMF (5 × 1 min), (ii) piperidine-DMF (1:1) (1 × 1 min + 2 × 15 min), (iii) DMF (5 × 1 min). In the cases where the Kaiser test was not a clear positive, an additional treatment with DBU:piperidine:toluene:DMF (5:5:20:70) (1 × 10 min) was performed.

Alloc Group Removal. Alloc group removal involved the following sequence: (i) Pd(PPh$_3$)$_4$ (0.1 equiv) and PhSiH$_3$ (10 equiv) in anhydrous DCM (3 × 15 min), (ii) anhydrous DCM (5 × 1 min), (iii) DCM (5 × 1 min), (iv) DMF (5 × 1 min), and (v) 0.02 M solution of sodium diethyldithiocarbamate in DMF (3 × 15 min), DMF (5 × 1 min), DCM (5 × 1 min), and DMF (5 × 1 min).

Analysis by RP-HPLC and RP-HPLC-MS. Crudes were analyzed by RP-HPLC-MS. The purified compounds were characterized by analytical RP-HPLC and RP-HPLC-MS using two different reverse-phase C$_{18}$ columns and flow 1 mL/min in two separate elution systems at 254 nm. RP-HPLC-MS conditions (method A): symmetry C$_{18}$ (3.5 μM, 4.6 mm × 75 mm,)

column, gradient 5% to 60% B in 7 min; A: H$_2$O-HCOOH (99.9:0.1); B: CH$_3$CN-HCOOH (99.3:0.7). RP-HPLC conditions (method B): X-Terra MS C$_{18}$, (3.5 μm, 4.6 mm × 100 mm) column, gradient 0% to 70% B in 10 min; A: H$_2$O-TFA (99.9:0.1); B: CH$_3$CN-TFA (99.9:0.1). Method A has been used to determine the purity of final compounds. HPLC data and purities of compounds **3–26** are included in Table 1 (SI).

Purification by Preparative RP-HPLC-MS. Monovalent and heterobivalent ligands were purified by preparative RP-HPLC-MS using different linear gradients of H$_2$O (containing 0.1% HCOOH) and CH$_3$CN (containing 0.07% HCOOH) at a flow rate of 25 mL/min. Column: symmetry C$_{18}$, 5 μm, 30 mm × 100 mm.

General Protocol for the Synthesis of Monovalent Ligands (11–26) and Heterobivalent (3–10) Ligands. Fmoc-NH-AM-MBHA resin (5 g, $f = 0.61$ mmol/g) was previously swelled with DCM (1 × 1 min, 2 × 10 min) and DMF (5 × 1 min, 1 × 15 min) before use and treated with piperidine as described before. After washings, the coupling mixture of Fmoc-L-Lys(Alloc)-OH (3 equiv), HOBt (3 equiv), and DIPCDI (3 equiv) in DMF was added to the resin and the resulting mixture was stirred for 2 h. The resin was washed and the Fmoc group removed yielding NH$_2$-L-Lys(Alloc)-AM-MBHA. At this point, a portion of resin (450 mg) was separated and divided on three aliquots of 150 mg to continue the synthesis of monovalent (**11**, **19**) and heterobivalent (**3**) ligands corresponding to spacer length $n = 0$.

The linker Fmoc-PEG-based unit (2.5 equiv, **39**) was introduced using PyBOP (2.5 equiv) and DIEA (5 equiv) and HOAt (2.5 equiv) as coupling reagents in DMF for 5 h at 25 °C. An acylation step was performed when the coupling was not completed. The three-step cycle (Fmoc elimination, Fmoc-PEG-based unit coupling, acylation) was repeated seven times, adding a repeating monomeric unit to the oligomeric chain. After each cycle, a portion of oligomeric resin (150–200 mg) was separated to continue the synthesis of the different lengths of monovalent and heterobivalent ligands (from $n = 1$ to $n = 7$).

Each aliquot of resin corresponding to each monovalent or heterobivalent precursor was washed and a mixture of Ac-L-Lys(Fmoc)-OH (3 equiv), PyBOP (3 equiv), HOAt (3 equiv), and DIEA (6 equiv) in DMF was added. The coupling mixtures were then stirred for 4 h at 25 °C. The resins were washed and the ε-NH-Fmoc group was then removed by following the procedure described previously. From this point onward, monovalent and heterobivalent ligand synthesis was continued separately.

Synthesis of XCC Monovalent Ligands (11–18). Boc-L-Lys-(Fmoc)-OH (2.1 g, 3 equiv), PyBOP (3 equiv), HOAt (3 equiv), and DIEA (6 equiv) were dissolved in DMF and added to each XCC monovalent ligand precursor resin ($n = 0$–7). Once the coupling was finished, the Fmoc group was removed in each case as described before and **1** (3 equiv), PyBOP (3 equiv), HOAt (3 equiv), and DIEA (6 equiv) in DMF were added. The mixture was then stirred for 4 h. The ε-NH-Alloc group was then eliminated as described previously followed by acetylation by treatment with Ac$_2$O (5 equiv) and DIEA (10 equiv) in DCM for 30 min. Finally, ligands **11–18** were cleaved from their corresponding resins with TFA:H$_2$O (95:5, v/v, 2 mL) for 1 h. The solvent was evaporated to dryness. Compounds **11–18** were purified by preparative RP-HPLC-MS using a linear gradient 10–50% CH$_3$CN for 30 min. Purities of all final compounds were ≥95% (see SI, Table 1).

(**11**). Amount of crude product: 21.4 mg. Purification gave 4.1 mg of pure **11**. (ES$^+$) calcd for C$_{41}$H$_{63}$N$_{11}$O$_9$, 853.48; found [M + H] = 854.7, [M + 2H/2] = 427.5.

(**12**). Amount of crude product: 31.5 mg. Purification gave 17 mg of pure **12**. (ES$^+$) calcd for C$_{56}$H$_{91}$N$_{13}$O$_{14}$, 1083.6; found [M + H] = 1084.8, [M + 2H/2] = 543.1.

(**13**). Amount of crude product: 40 mg. Purification gave 3.0 mg of pure **13**. (ES$^+$) calcd for C$_{71}$H$_{119}$N$_{15}$O$_{19}$, 1313.7; found [M + H] = 1315.0, [M + 2H/2] = 658.2.

(14). Amount of crude product: 23.6 mg. Purification gave 2.1 mg of pure **14**. (ES$^+$) calcd for $C_{86}H_{147}N_{17}O_{24}$, 1544.79; found [M + H] = 1546.2, [M + 2H/2] = 773.5, [M + 2H/2] = 516.0.

(15). Amount of crude product: 48 mg. Purification gave 17.0 mg of pure **15**. (ES$^+$) calcd for $C_{102}H_{177}N_{19}O_{28}$, 1775.1; found [M + H] = 1777.0, [M + 2H/2] = 888.7, [M + 3H/3] = 592.9.

(16). Amount of crude product: 54 mg. Purification gave 29.3 mg of pure **16**. (ES$^+$) calcd for $C_{116}H_{203}N_{21}O_{34}$, 2005.31; found [M + H] = 2007.1, [M + 2H/2] = 1003.9, [M + 3H/3] = 669.6.

(17). Amount of crude product: 63 mg. Purification gave pure 23.7 mg of **17**. (ES$^+$) calcd for $C_{131}H_{231}N_{23}O_{39}$, 2236.06; found [M + 2H/2] = 1119.2, [M + 3H/3] = 746.5.

(18). Amount of crude product: 27.5 mg. Purification gave pure 1.2 mg of **18**. (ES$^+$) calcd for $C_{146}H_{259}N_{25}O_{44}$, 2465.83; found [M + 2H/2] = 1234.04, [M + 3H/3] = 823.05, [M + 4H/4] = 617.5.

Synthesis of Fmoc-L-Glu(γ-(±)-PPHT-NH$_2$)-OH (40). HOBt (1 equiv) and DIPCDI (1 equiv) were added to a solution of Fmoc-L-Glu-O^{t}Bu (642 mg) in DMF (10 mL). The reaction mixture was stirred for 5 min. Next, (±)-PPHT-NH$_2$ (**2**) (1equiv) was added and the reaction mixture was stirred for an additional 18 h. The solvent was concentrated in vacuo and the obtained solid was dissolved in DCM (25 mL) and washed with 5% NaHCO$_{3(aq)}$ (3 × 50 mL). The organic layer was dried over MgSO$_4$ and evaporated to dryness to yield Fmoc-L-Glu(γ-(±)-PPHT-NH$_2$)-O^{t}Bu (1.145 g, yield = 95%, purity 92% (RP-HPLC-MS conditions). (ES$^+$) calcd for $C_{45}H_{53}N_3O_6$, 731.39; found [M + H] = 732.45.

Fmoc-L-Glu(γ-(±)-PPHT-NH$_2$)-OtBu (1.145 g) was suspended in 4 M HCl in dioxane (15 mL) and stirred for 4 h. The reaction mixture was concentrated in vacuo and coevaporated three times with dioxane and three times with H$_2$O:ACN (1:1, v/v) to yield Fmoc-L-Glu(γ-(±)-PPHT-NH$_2$)-OH as a brown solid (1.031 g, yield = 98%). The purity of **40** was 95% (RP-HPLC-MS conditions). (ES$^+$) calcd for $C_{41}H_{45}N_3O_6$, 675.33; found [M + H] = 676.33. The product was used without any further purification and characterization.

Synthesis of PPHT Monovalent Ligands (19−26). Each aliquot of resin that corresponded to each PPHT monovalent ligand ($n = 0−7$) were acetylated by treatment with Ac$_2$O (10 equiv) and DIEA (10 equiv) in DCM for 30 min. After that, the ε-NH-Alloc group was eliminated and a mixture of Fmoc-L-Glu(γ-(±)-PPHT-NH$_2$)-OH (3 equiv), HOBt (3 equiv), and DIPCDI (3 equiv) in DMF was added to each PPHT monovalent ligand precursor resin ($n = 0−7$). Finally, after Fmoc group removal, ligands **19−26** were cleaved from their corresponding resins with a mixture of TFA:H$_2$O (95:5, v/v, 2 mL) for 1 h. The solvent was evaporated to dryness. Products **19−26** were purified by preparative C18 RP-HPLC-MS using a linear gradient 0−50% CH$_3$CN in 30 min. Purities of all final compounds were ≥95% (see SI, Table 1) with the exception of compounds **21** (90%) and **26** (91%).

(19). Amount of crude product: 76 mg. Purification RP-HPLC-MS gave 2.3 mg of pure **19**. (ES$^+$) calcd for $C_{42}H_{64}N_8O_7$, 792.49; found [M + H] = 793.8, [M + 2H/2] = 397.5.

(20). Amount of crude product: 55 mg. Purification gave 3.6 mg of pure **20**. (ES$^+$) calcd for $C_{52}H_{82}N_{10}O_{11}$, 1022.62; found [M + H] = 1024.0, [M + 2H/2] = 512.8.

(21). Amount of crude product: 85 mg. Purification gave 3.2 mg pure **21**. (ES$^+$) calcd for $C_{62}H_{100}N_{12}O_{15}$, 1252.74; found [M + H] = 1254.1, [M + 2H/2] = 627.9, [M + 3H/3] = 418.9.

(22). Amount of crude product: 47 mg. Purification gave 4.9 mg of pure **22**. (ES$^+$) calcd for $C_{72}H_{118}N_{14}O_{19}$, 1482.87; found [M + H] = 1484.7, [M + 2H/2] = 743.1, [M + 3H/3] = 495.8, [M + 4H/4] = 372.1.

(23). Amount of crude product: 60 mg. Purification gave 0.7 mg of pure **23**. (ES$^+$) calcd for $C_{82}H_{136}N_{16}O_{23}$, 1713.00; found [M + H] = 1715.5, [M + 2H/2] = 858.2, [M + 3H/3] = 572.5.

(24). Amount of crude product: 95 mg. Purification gave 0.4 mg of pure **24**. (ES$^+$) calcd for $C_{92}H_{154}N_{18}O_{27}$, 1943.12; found [M + H] = 1945.5, [M + 2H/2] = 973.5, [M + 3H/3] = 649.4, [M + 4H/4] = 487.4.

(25). Amount of crude product: 103 mg. Purification gave 0.4 mg of pure **25**. (ES$^+$) calcd for $C_{102}H_{172}N_{20}O_{31}$, 2173.25; found [M + 2H/2] = 1088.4, [M + 3H/3] = 725.9, [M + 4H/4] = 544.8, [M + 4H/4] = 436.1.

(26). Amount of crude product: 69 mg. Purification gave 2.7 mg of pure **26**. (ES$^+$) calcd for $C_{112}H_{190}N_{22}O_{35}$, 2403.38; found [M + 2H/2] = 1203.0, [M + 3H/3] = 802.4, [M + 4H/4] = 602.3, [M + 4H/4] = 482.2.

Synthesis of XCC-PPHT Heterobivalent Ligands (3−10). Boc-L-Lys(Fmoc)-OH (3 equiv), HOBt (3 equiv), and DIPCDI (3 equiv) in DMF were added to each heterobivalent ligand precursor resin ($n = 0−7$), and the resulting mixture was stirred for 2 h. After washings, the Fmoc group was removed in each case, **1** (3 equiv), PyBOP (3 equiv), HOAt (3 equiv), and DIEA (6 equiv) were added, and the mixture stirred for 4 h. After elimination of ε-NH-Alloc, a mixture of Fmoc-L-Glu(γ-(±)-PPHT-NH$_2$)-OH (3 equiv), PyBOP (3 equiv), HOAt (3 equiv), and DIEA (6 equiv) in DMF was added to each heterobivalent ligand precursor resin. Once the reaction was finished, the Fmoc group was eliminated and subsequently followed by cleavage of ligands **3−10** from their resins with a mixture of TFA:H$_2$O (95:5, v/v, 2 mL) for 1 h. The solvent was evaporated to dryness. Products **3−10** were purified by preparative HPLC-MS using a linear gradient 0−50% CH$_3$CN in 30 min. Purities of all final compounds were ≥95% (see SI, Table 1).

(3). Amount of crude product: 171 mg. Purification gave 20.8 mg of pure **3**. (ES$^+$) calcd for $C_{65}H_{94}N_{14}O_{11}$, 1246.72; found [M + H] = 1248.7, [M + 2H/2] = 624.9, [M + 3H/3] = 417.0.

(4). Amount of crude product: 64.0 mg. Purification gave 12.1 mg of pure **4**. Purity: 99%. (ES$^+$) calcd for $C_{75}H_{112}N_{16}O_{15}$, 1476.85; found [M + H] = 1479.4, [M + 2H/2] = 740.0, [M + 3H/3] = 493.8.

(5). Amount of crude product: 84.0 mg. Purification gave 4.9 mg of pure **5**. (ES$^+$) calcd for $C_{85}H_{130}N_{18}O_{19}$, 1706.98; found [M + H] = 1708.7, [M + 2H/2] = 855.0, [M + 3H/3] = 570.4, [M + 4H/4] = 428.2.

(6). Amount of crude product: 63.1 mg. Purification gave 5.8 mg of pure **6**. (ES$^+$) calcd for $C_{95}H_{148}N_{20}O_{23}$, 1937.10; found [M + H] = 1940.0, [M + 2H/2] = 970.2, [M + 3H/3] = 647.1, [M + 4H/4] = 485.8.

(7). Amount of crude product: 65.9 mg. Purification gave 4.8 mg of pure **7**. (ES$^+$) calcd for $C_{105}H_{166}N_{22}O_{27}$, 2167.23; found [M + H] = 2169.6, [M + 2H/2] = 1085.2, [M + 3H/3] = 723.9, [M + 4H/4] = 543.2.

(8). Amount of crude product: 103.2 mg. Purification gave 2.5 mg of pure **8**. (ES$^+$) calcd for $C_{115}H_{184}N_{24}O_{31}$, 2397.36; found [M + 2H/2] = 1200.4, [M + 3H/3] = 800.7, [M + 4H/4] = 600.8, [M + 5H/5] = 481.0.

(9). Amount of crude product: 106.0 mg. Purification gave 2.6 mg of pure **9**. (ES$^+$) calcd for $C_{125}H_{202}N_{26}O_{35}$, 2627.48; found [M + 2H/2] = 1315.6, [M + 3H/3] = 877.4, [M + 4H/4] = 658.3, [M + 5H/5] = 527.1, [M + 6H/6] = 439.4.

(10). Amount of crude product: 125.3 mg. Purification gave 1.1 mg of pure **10**. (ES$^+$) calcd for $C_{135}H_{220}N_{28}O_{39}$, 2857.61; found [M + 2H/2] = 1431.2, [M + 3H/3] = 954.2, [M + 4H/4] = 715.9, [M + 5H/5] = 573.1, [M + 6H/6] = 477.9.

Docking Experiments. The D$_2$−A$_{2A}$ receptor heterodimer in the present computational experiments belongs to the cluster of docking solutions achieved in previous studies.[12] It resembles the semiempirical model of dimeric rhodopsin.[50] In this model, the heterodimer interface is mainly formed by the second intracellular loop (I2), helices 4, 3, and 5 from D$_2$R, and I2, helices 5, 3, and 4 from A$_{2A}$R. Compound **3** was manually docked into the putative binding sites of the two receptors by probing slightly different conformations of the ligand and the receptor side chains. The docking criteria were aimed

at: (a) allowing the formation of salt bridge interactions between all the three protonated amino groups of the ligand and anionic sites of the dimeric receptor, (b) causing all the polar atoms of the ligand to be engaged in H-bonding interactions, and (c) allowing for the accomplishment of a few critical interactions between the dopamine part of the ligand and the D_2R. These interactions included: the charge-reinforced H-bond between (a) the protonated nitrogen atom of PPTH moiety and D114 in helix 3 of D_2R, and (b) an H-bond between the hydroxyl group of PPTH moiety and S197 in helix 5 of D_2R. The probed complexes between the receptor heterodimer and the bivalent ligand were subjected to energy refinement through 100 ps of balanced Molecular Dynamics simulations, following the same computational protocol employed to refine monomeric D_2R and A_2R models.[12] For each complex, the structures averaged over the 200 structures collected during the last 100 ps of the balanced MD trajectory were minimized and subjected to structural analysis. As a last step, the complex characterized by the best ligand−receptor complementarity was finally selected. We considered also two alternative heterodimers made by a β_2-AR-based model of D_2R (PDB code: 2RH1)[47] and the crystal structure of $A_{2A}R$[48] (PDB code: 3EML) (see SI Figures 2 and 3). Predictions of the two heterodimers were based on a well-established protocol.[51,52] Refinement of the D_2R and of the heterodimer receptors−**3** complexes was carried out by employing the GBSW implicit water/membrane water implemented in CHARMM.[53]

Cell Culture and Transfection. Human embryonic kidney-293 (HEK-293) cell line and mouse fibroblast Ltk cell line were cultured in Dulbecco's modified Eagle's medium (DMEM) with 4.5 mg/mL glucose and 0.11 mg/mL sodium pyruvate supplemented with 10% fetal bovine serum, 100 units/mL penicillin, 100 μg/mL streptomycin, and 2 mM L-glutamine at 37 °C in a humidified atmosphere of 5% CO_2. For binding experiments, mouse fibroblast Ltk cells were seeded in 150 mm dishes and transiently transfected with cDNA corresponding to human $A_{2A}R$ or human D_2R (long isoform) or both cDNAs at the same time. For cAMP experiments, HEK-293 cells were grown in 25 cm^2 flasks and transiently transfected with the human cDNA encoding for $A_{2A}R$ or D_2R. Tranfections were performed using the Lipofectamine 2000 reagent kit according to the manufacturer's instructions. HEK-293 cells transiently expressing $A_{2A}R$ or $D_{2L}R$ were incubated in serum-free medium in the presence of 1.5 U/mL ADA for cells expressing $A_{2A}R$, 16 h before the experiment.

Membrane Preparation and Protein Determination. Membrane suspensions from lamb brain striatum were prepared as described previously.[54] Tissue was disrupted with a Polytron homogenizer for three 10 s periods in 10 volumes of ice-cold Tris-HCl buffer (50 mM, pH 7.4), containing a protease inhibitor cocktail. Membranes were obtained by centrifugation at 105000g for 40 min at 4 °C, and the pellet was resuspended and recentrifuged under the same conditions. The resulting pellet was stored at −80 °C and was washed once more as described above and resuspended in Tris-HCl buffer (50 mM, pH 7.4) for immediate use. Protein was quantified by the bicinchoninic acid method using bovine serum albumin dilutions as the standard. Mouse fibroblast Ltk cells were lifted from dishes with a cell scraper 48 h after transfection and harvested by centrifugation at 1500g for 5 min. Cell pellet was washed twice with PBS and resuspended in 10 volumes of ice-cold Tris-HCl buffer (50 mM, pH 7.4). Cell suspension was disrupted with a Polytron homogenizer for three 10 s periods, and the homogenates were processed as described above for striatum membranes.

Radioligand Binding Experiments. Competition experiments were performed by incubating (2 h) membranes (0.3−0.5 mg of protein/mL) at 25 °C in Tris-HCl buffer (50 mM, pH 7.4) containing 10 mM $MgCl_2$ and 2 U/mL adenosine deaminase (ADA) with the indicated concentrations of the $A_{2A}R$ antagonist [³H]ZM-241385 or the D_2R or antagonist [³H]YM-09151-2.

Screenings were performed in the absence or presence of non-labeled compounds at a unique concentration of 1 μM and for displacement curves in the absence or presence of increasing concentrations of nonlabeled compounds (triplicates of 11 different displacer concentrations from 0.1 nM to 50 μM). Nonspecific binding was determined in the presence of 50 μM ZM-241385 for $A_{2A}R$ or 50 μM YM-09151-2 for D_2R and, in competition experiments, it was confirmed that the value was the same as calculated by extrapolation of the competition curves. Free and membrane-bound ligand were separated by rapid filtration of 500 μL aliquots in a Brandel cell harvester trough Wathman GF/C filters embedded in 0.3% polyethylenimine. Filters were washed in 5 mL of ice-cold Tris-HCl buffer (50 mM, pH 7.4) and transferred in vials containing 10 mL of Ecoscint H scintillation cocktail. After overnight shaking, radioactivity counts were determined using a Packard 1600 TRI-CARB scintillation counter with an efficiency of 62%.[54] Binding data from competition experiments were analyzed by nonlinear regression using the commercial Grafit curve-fitting software by fitting the binding data to the two-state dimer receptor model.[35,36] To calculate the macroscopic equilibrium dissociation constants involved in the binding of the compounds to the dimer as a whole, the new equations deduced by Casadó et al. were employed.[37] The macroscopic equilibrium dissociation constants involved in the binding of the agonists were calculated following eq 1[37] below:

$$A_{bound} = (K_{DA2}A + 2A^2 + K_{DA2}AB/K_{DAB})R_T/(K_{DA1}K_{DA2}$$
$$+ K_{DA2}A + A^2 + K_{DA2}AB/K_{DAB} + K_{DA1}K_{DA2}B/K_{DB1}$$
$$+ K_{DA1}K_{DA2}B^2/(K_{DB1}K_{DB2})) \quad (1)$$

where A represents the radioligand (the dopamine D_2 receptor antagonist [³H]YM-09151-2 or the adenosine A_{2A} receptor antagonist [³H]ZM 241385) concentration, R_T is the total amount of receptor dimers, and K_{DA1} and K_{DA2} are the macroscopic dissociation constants describing the binding of the first and the second radioligand molecule (A) to the dimeric receptor. B represents the assayed competing compound concentration, and K_{DB1} and K_{DB2} are, respectively, the equilibrium dissociation constants of the first and second binding of B; K_{DAB} can be described as a hybrid equilibrium radioligand/competitor dissociation constant, which is the dissociation constant of B binding to a receptor dimer semioccupied by A.

Because the radioligand A (the dopamine D_2 receptor antagonist [³H]YM-09151-2 or the adenosine A_{2A} receptor antagonist [³H]ZM 241385) showed noncooperative behavior, eq 1 was simplified to eq 2 due to the fact that $K_{DA2} = 4K_{DA1}$:[37]

$$A_{bound} = (4K_{DA1}A + 2A^2 + 4K_{DA1}AB/K_{DAB})R_T/(4K_{DA1}^2$$
$$+ 4K_{DA1}A + A^2 + 4K_{DA1}AB/K_{DAB} + 4K_{DA1}^2B/K_{DB1}$$
$$+ 4K_{DA1}^2B^2/(K_{DB1}K_{DB2})) \quad (2)$$

The dimer cooperativity index for the competing ligand B37 was calculated following eq 3:[37]

$$D_C = \log(4K_{DB1}/K_{DB2}) \quad (3)$$

D_C would be a measure of ligand homotropic cooperativity. It measures the orthosteric dissociation equilibrium constant value modifications occurring when a protomer senses the binding of the same ligand molecule to the partner protomer (in a dimer). The way the index is defined is such that its value is "0" when the binding of the first molecule of ligand to one protomer of the empty dimer does not affect the binding of the second molecule to the empty protomer in the dimer. Positive or negative values of D_c indicate that the presence of the first bound molecule increases or decreases respectively the affinity for binding of the second molecule to the empty protomer in the dimer.[37]

Goodness of fit was tested according to a reduced χ^2 value given by the nonlinear regression program. The test of

significance for two different population variance models was based upon the F distribution.[54] Using this F test, a probability greater than 95% ($p < 0.05$) was considered the criterion to select a more complex model (cooperativity) over the simplest one (noncooperativity). In all cases, a probability of less than 70% ($p > 0.30$) resulted when one model was not significantly better than the other.

cAMP Determination. HEK-293 cells, 48 h after transfection, were preincubated with 50 μM zardaverine as phosphodiesterase inhibitor for 10 min at 37 °C in serum-free medium containing 10 mM MgCl$_2$ and 1.5 U/mL ADA (for A$_{2A}$R). The ligands were added sequentially at the concentrations indicated: 10 min antagonists, 10−15 min agonists, and 15 min forskolin.

To stop the reaction, the cells were placed on ice, detached, and washed twice in ice-cold PBS. After centrifugation at 2500g for 5 min at 4 °C, the pellet was resuspended with 200 μL ice-cold HClO$_4$ (4%) for 30 min and 1.5 M KOH was added to reach neutral pH. Samples were centrifuged at 15000g for 30 min at 4 °C and the supernatant was frozen at −20 °C. The accumulation of cAMP in the samples was measured by a [^{3}H] cAMP assay system as described in the manual from the manufacturer.

Supporting Information Available: Molecular docking studies, experimental description of the synthesis and characterization of compounds **1**, **2**, and **39** and its intermediates, table containing **3**−**26** compound purities determined by HPLC, ^{1}H, and ^{13}C NMR spectra and HPLC chromatograms of compounds **1**, **2**, and **39** and its intermediates, and **3**−**26** compound HPLC chromatograms. This material is available free of charge via the Internet at http://pubs.acs.org.

References

(1) Bouvier, M. Oligomerization of G-protein-coupled transmitter receptors. *Nat. Rev. Neurosci.* **2001**, *2*, 274–286.

(2) Park, P. S.; Filipek, S.; Wells, J. W.; Palczewski, K. Oligomerization of G protein-coupled receptors: past, present, and future. *Biochemistry* **2004**, *43*, 15643–15656.

(3) Fuxe, K.; Canals, M.; Torvinen, M.; Marcellino, D.; Terasmaa, A.; Genedani, S.; Leo, G.; Guidolin, D.; az-Cabiale, Z.; Rivera, A.; Lundstrom, L.; Langel, U.; Narvaez, J.; Tanganelli, S.; Lluís, C.; Ferré, S.; Woods, A.; Franco, R.; Agnati, L. F. Intramembrane receptor–receptor interactions: a novel principle in molecular medicine. *J. Neural Transm.* **2007**, *114*, 49–75.

(4) Carriba, P.; Navarro, G.; Ciruela, F.; Ferré, S.; Casadó, V.; Agnati, L.; Cortés, A.; Mallol, J.; Fuxe, K.; Canela, E. I.; Lluís, C.; Franco, R. Detection of heteromerization of more than two proteins by sequential BRET-FRET. *Nat. Methods* **2008**, *5*, 727–733.

(5) Jordan, B. A.; Devi, L. A. G-protein-coupled receptor heterodimerization modulates receptor function. *Nature* **1999**, *399*, 697–700.

(6) Terrillon, S.; Bouvier, M. Roles of G-protein-coupled receptor dimerization. *EMBO Rep.* **2004**, *5*, 30–34.

(7) Prinster, S. C.; Hague, C.; Hall, R. A. Heterodimerization of G protein-coupled receptors: specificity and functional significance. *Pharmacol. Rev.* **2005**, *57*, 289–298.

(8) George, S. R.; O'Dowd, B. F.; Lee, S. P. G-protein-coupled receptor oligomerization and its potential for drug discovery. *Nat. Rev. Drug Discovery* **2002**, *1*, 808–820.

(9) Maggio, R.; Novi, F.; Scarselli, M.; Corsini, G. U. The impact of G-protein-coupled receptor hetero-oligomerization on function and pharmacology. *FEBS J.* **2005**, *272*, 2939–2946.

(10) Milligan, G. G-protein-coupled receptor heterodimers: pharmacology, function and relevance to drug discovery. *Drug Discovery Today* **2006**, *11*, 541–549.

(11) Hillion, J.; Canals, M.; Torvinen, M.; Casadó, V.; Scott, R.; Terasmaa, A.; Hansson, A.; Watson, S.; Olah, M. E.; Mallol, J.; Canela, E. I.; Zoli, M.; Agnati, L. F.; Ibanez, C. F.; Lluís, C.; Franco, R.; Ferré, S.; Fuxe, K. Coaggregation, cointernalization, and codesensitization of adenosine A$_{2A}$ receptors and dopamine D$_2$ receptors. *J. Biol. Chem.* **2002**, *277*, 18091–18097.

(12) Canals, M.; Marcellino, D.; Fanelli, F.; Ciruela, F.; de Benedetti, P.; Goldberg, S. R.; Neve, K.; Fuxe, K.; Agnati, L. F.; Woods, A. S.; Ferré, S.; Lluís, C.; Bouvier, M.; Franco, R. Adenosine A$_{2A}$-dopamine D$_2$ receptor-receptor heteromerization: qualitative and quantitative assessment by fluorescence and bioluminescence energy transfer. *J. Biol. Chem.* **2003**, *278*, 46741–46749.

(13) Kamiya, T.; Saitoh, O.; Yoshioka, K.; Nakata, H. Oligomerization of adenosine A$_{2A}$ and dopamine D$_2$ receptors in living cells. *Biochem. Biophys. Res. Commun.* **2003**, *306*, 544–549.

(14) Agnati, L. F.; Ferré, S.; Lluís, C.; Franco, R.; Fuxe, K. *Pharmacol. Rev.* **2003**, *55*, 509–550.

(15) Ferré, S.; Fredholm, B. B.; Morelli, M.; Popoli, P.; Fuxe, K. Adenosine−dopamine receptor−receptor interactions as an integrative mechanism in the basal ganglia. *Trends Neurosci.* **1997**, *20*, 482–487.

(16) Ferré, S; Ciruela, F; Woods, A. S.; Canals, M; Burgueño, J; Marcellino, D; Karcz-Kubicha, M; Hope, B. T.; Morales, M; Popoli, P; Goldberg, S. R.; Fuxe, K; Lluís, C; Franco, R; Agnati, L. F. Glutamate mGlu$_5$-adenosine A$_{2A}$-dopamine D$_2$ receptor interactions in the striatum. Implications for drug therapy in neuropsychiatric disorders and drug abuse. *Curr. Med. Chem.* **2003**, *3*, 1–26.

(17) Schiffmann, S. N.; Jacobs, O.; Vanderhaeghen, J. J. Striatal restricted adenosine A$_2$ receptor (RDC8) is expressed by enkephalin but not by substance P neurons: an in situ hybridization histochemistry study. *J. Neurochem.* **1991**, *57*, 1062–1067.

(18) Fink, J. S.; Weaver, D. R.; Rivkees, S. A.; Peterfreund, R. A.; Pollack, A. E.; Adler, E. M.; Reppert, S. M. Molecular cloning of the rat A$_2$ adenosine receptor: selective co-expression with D$_2$ dopamine receptors in rat striatum. *Brain Res. Mol. Brain Res.* **1992**, *14*, 186–195.

(19) Ferré, S.; Ciruela, F.; Canals, M.; Marcellino, D.; Burgueño, J.; Casadó, V.; Hillion, J.; Torvinen, M.; Fanelli, F.; de Benedetti, P.; Goldberg, S. R.; Bouvier, M.; Fuxe, K.; Agnati, L. F.; Lluís, C.; Franco, R.; Woods, A. Adenosine A$_{2A}$-dopamine D$_2$ receptor-receptor heteromers. Targets for neuropsychiatric disorders. *Parkinsonism Relat. Disord.* **2004**, *10*, 265–271.

(20) Fuxe, K.; Ferré, S.; Genedani, S.; Franco, R.; Agnati, L. F. Adenosine receptor−dopamine receptor interactions in the basal ganglia and their relevance for brain function. *Physiol. Behav.* **2007**, *92*, 210–217.

(21) Ferré, S.; Fuxe, K.; von, E. G.; Johansson, B.; Fredholm, B. B. Adenosine−dopamine interactions in the brain. *Neuroscience* **1992**, *51*, 501–512.

(22) Bara-Jimenez, W.; Sherzai, A.; Dimitrova, T.; Favit, A.; Bibbiani, F.; Gillespie, M.; Morris, M. J.; Mouradian, M. M.; Chase, T. N. Adenosine A(2A) receptor antagonist treatment of Parkinson's disease. *Neurology* **2003**, *61*, 293–296.

(23) Hauser, R. A.; Hubble, J. P.; Truong, D. D. Randomized trial of the adenosine A$_{2A}$ receptor antagonist istradefylline in advanced PD. *Neurology* **2003**, *61*, 297–303.

(24) Schwarzschild, M. A.; Agnati, L.; Fuxe, K.; Chen, J. F.; Morelli, M. Targeting adenosine A$_{2A}$ receptors in Parkinson's disease. *Trends Neurosci.* **2006**, *29*, 647–654.

(25) Jacobson, K. A.; Xie, R.; Young, L.; Chang, L.; Liang, B. T. A novel pharmacological approach to treating cardiac ischemia. Binary conjugates of A$_1$ and A$_3$ adenosine receptor agonists. *J. Biol. Chem.* **2000**, *275*, 30272–30279.

(26) Daniels, D. J.; Lenard, N. R.; Etienne, C. L.; Law, P. Y.; Roerig, S. C.; Portoghese, P. S. Opioid-induced tolerance and dependence in mice is modulated by the distance between pharmacophores in a bivalent ligand series. *Proc. Natl. Acad. Sci. U.S.A.* **2005**, *102*, 19208–19213.

(27) Jacobson, K. A.; Kirk, K. L.; Padgett, W. L.; Daly, J. W. Functionalized Congeners of 1,3-Dialkylxanthines—Preparation of Analogs with High-Affinity for Adenosine Receptors. *J. Med. Chem.* **1985**, *28*, 1334–1340.

(28) Bakthavachalam, V.; Baindur, N.; Madras, B. K.; Neumeyer, J. L. Fluorescent-probes for dopamine receptors—Synthesis and characterization of fluorescein and 7-nitrobenz-2-oxa-1,3-diazol-4yl conjugates of D$_1$ and D$_2$ receptor ligands. *J. Med. Chem.* **1991**, *34*, 3235–3241.

(29) Horn, A. S.; Tepper, P.; Kebabian, J. W.; Beart, P. M. N-0434, a very potent and specific new D_2 dopamine receptor agonist. *Eur. J. Pharmacol*. **1984**, *99*, 125–126.

(30) Unpublished results.

(31) Song, A.; Zhang, J.; Lebrilla, C. B.; Lam, K. S. A novel and rapid encoding method based on mass spectrometry for "one-bead-one-compound" small molecule combinatorial libraries. *J. Am. Chem. Soc*. **2003**, *125*, 6180–6188.

(32) Fuxe, K.; Marcellino, D.; Genedani, S.; Agnati, L. Adenosine A_{2A} receptors, dopamine D_2 receptors and their interactions in Parkinson's disease. *Movement Disord*. **2007**, *22*, 1990–2017.

(33) Canals, M.; Burgueño, J.; Marcellino, D.; Cabello, N.; Canela, E. I.; Mallol, J.; Agnati, L.; Ferré, S.; Bouvier, M.; Fuxe, K.; Ciruela, F.; Lluís, C.; Franco, R. Homodimerization of adenosine A_{2A} receptors: qualitative and quantitative assessment by fluorescence and bioluminescence energy transfer. *J. Neurochem*. **2004**, *88*, 726–734.

(34) Lee, S. P.; O'Dowd, B. F.; Rajaram, R. D.; Nguyen, T.; George, S. R. D_2 dopamine receptor homodimerization is mediated by multiple sites of interaction, including an intermolecular interaction involving transmembrane domain 4. *Biochemistry* **2003**, *42*, 11023–11031.

(35) Franco, R.; Casadó, V.; Mallol, J.; Ferré, S.; Fuxe, K.; Cortés, A.; Ciruela, F.; Lluís, C.; Canela, E. I. Dimer-based model for heptaspanning membrane receptors. *Trends Biochem. Sci*. **2005**, *30*, 360–366.

(36) Franco, R.; Casadó, V.; Mallol, J.; Ferrada, C.; Ferré, S.; Fuxe, K.; Cortés, A.; Ciruela, F.; Lluís, C.; Canela, E. I. The two-state dimer receptor model: a general model for receptor dimers. *Mol. Pharmacol*. **2006**, *69*, 1905–1912.

(37) Casadó, V.; Cortés, A.; Ciruela, F.; Mallol, J.; Ferré, S.; Lluís, C.; Canela, E. I.; Franco, R. Old and new ways to calculate the affinity of agonists and antagonists interacting with G-protein-coupled monomeric and dimeric receptors: the receptor−dimer cooperativity index. *Pharmacol. Ther*. **2007**, *116*, 343–354.

(38) Franco, R.; Casadó, V.; Cortés, A.; Mallol, J.; Ciruela, F.; Ferré, S.; Lluís, C.; Canela, E. I. G-protein-coupled receptor heteromers: function and ligand pharmacology. *Br. J. Pharmacol*. **2008**, *153* (Suppl 1), S90–S98.

(39) Maggio, R.; Innamorati, G.; Parenti, M. G protein-coupled receptor oligomerization provides the framework for signal discrimination. *J. Neurochem*. **2007**, *103*, 1741–1752.

(40) Portoghese, P. S. From models to molecules: opioid receptor dimers, bivalent ligands, and selective opioid receptor probes. *J. Med. Chem*. **2001**, *44*, 2259–2269.

(41) Bhushan, R. G.; Sharma, S. K.; Xie, Z.; Daniels, D. J.; Portoghese, P. S. A bivalent ligand (KDN-21) reveals spinal delta and kappa opioid receptors are organized as heterodimers that give rise to delta(1) and kappa(2) phenotypes. Selective targeting of delta−kappa heterodimers. *J. Med. Chem*. **2004**, *47*, 2969–2972.

(42) Halazy, S.; Perez, M.; Fourrier, C.; Pallard, I.; Pauwels, P. J.; Palmier, C.; John, G. W.; Valentin, J. P.; Bonnafous, R.; Martinez, J. Serotonin dimers: application of the bivalent ligand approach to the design of new potent and selective 5-HT(1B/1D) agonists. *J. Med. Chem*. **1996**, *39*, 4920–4927.

(43) Russo, O.; Berthouze, M.; Giner, M.; Soulier, J. L.; Rivail, L.; Sicsic, S.; Lezoualc'h, F.; Jockers, R.; Berque-Bestel, I. Synthesis of specific bivalent probes that functionally interact with 5-HT(4) receptor dimers. *J. Med. Chem*. **2007**, *50*, 4482–4492.

(44) Christopoulos, A.; Grant, M. K.; Ayoubzadeh, N.; Kim, O. N.; Sauerberg, P.; Jeppesen, L.; El-Fakahany, E. E. Synthesis and pharmacological evaluation of dimeric muscarinic acetylcholine receptor agonists. *J. Pharmacol. Exp. Ther*. **2001**, *298*, 1260–1268.

(45) Vagner, J.; Xu, L.; Handl, H. L.; Josan, J. S.; Morse, D. L.; Mash, E. A.; Gillies, R. J.; Hruby, V. J. Heterobivalent ligands crosslink multiple cell-surface receptors: the human melanocortin-4 and delta-opioid receptors. *Angew. Chem., Int. Ed*. **2008**, *47*, 1685–1688.

(46) Handl, H. L.; Sankaranarayanan, R.; Josan, J. S.; Vagner, J.; Mash, E. A.; Gillies, R. J.; Hruby, V. J. Synthesis and evaluation of bivalent NDP-alpha-MSH(7) peptide ligands for binding to the human melanocortin receptor 4 (hMC4R). *Bioconjugate Chem*. **2007**, *18*, 1101–1109.

(47) Rosenbaum, D. M.; Cherezov, V.; Hanson, M. A.; Rasmussen, S. G. F.; Thian, F. S.; Kobilka, T. S.; Choi, H.-J.; Yao, X.-J.; Weis, W. I.; Stevens, R. C.; Kobilka, B. K. GPCR engineering yields high-resolution structural insights into β_2-adrenergic receptor function. *Science* **2007**, *318*, 1266–1273.

(48) Jaaloka, V.-P.; Griffith, M. T.; Hanson, M. A.; Cherezov, V.; Chien, E. Y. T.; Lane, J. R.; Ijzerman, A. P.; Stevens, R. C. The 2.6 Angstrom crystal structure of a human A_{2A} receptor bound to an agonist. *Science* **2008**, *322*, 1212–1217.

(49) Milligan, G.; Bouvier, M. Methods to monitor the quaternary structure of G-protein-coupled receptors. *FEBS J*. **2005**, *272*, 2914–2925.

(50) Liang, Y.; Fotiadis, D.; Filipek, S.; Saperstein, D. A.; Palczewski, K.; Engel, A. Organization of the G-protein-coupled receptors rhodopsin and opsin in native membranes. *J. Biol. Chem*. **2003**, *278*, 21655–21662.

(51) Casciari, D.; Seeber, M.; Fanelli, F. Quaternary structure predictions of transmembrane proteins starting from the monomer: a docking-base approach. *BMC Bioinformatics* **2006**, *7*, 340–355.

(52) Casciari, D.; Dell'Orco, D.; Fanelli, F. Homodimerization in Neurotensin 1 receptor involves helices 1, 2 and 4: insights form quaternary structure predictions and dimerization free energy estimations. *J. Chem. Inf. Model*. **2008**, *48*, 1669–1678.

(53) Im, W.; Feig, M.; Brooks, C. W., III An implicit membrane generalizaed born theory for the study of the structure, stability, and interactions of membrane proteins. *Biophys. J*. **2003**, *85*, 2900–2918.

(54) Casadó, V.; Canti, C.; Mallol, J.; Canela, E. I.; Lluís, C.; Franco, R. Solubilization of A_1 adenosine receptor from pig brain: characterization and evidence of the role of the cell membrane on the coexistence of high- and low-affinity states. *J. Neurosci. Res*. **1990**, *26*, 461–473.